

CALL FOR PAPERS | *Chronic Kidney Disease and Fibrosis*

## Nuclear factor of activated T cells mediates RhoA-induced fibronectin upregulation in glomerular podocytes

Lei Zhu,<sup>1</sup> Xiao-Yan Qi,<sup>2</sup> Lamine Aoudjit,<sup>1</sup> Flaviana Mouawad,<sup>1</sup> Cindy Baldwin,<sup>1</sup> Stanley Nattel,<sup>2</sup> and Tomoko Takano<sup>1</sup>

<sup>1</sup>Department of Medicine, McGill University Health Centre, Montreal, Quebec, Canada; and <sup>2</sup>Department of Medicine and Research Center, Montreal Heart Institute and Université de Montréal, Montreal, Quebec, Canada

Submitted 27 August 2012; accepted in final form 4 February 2013

**Zhu L, Qi XY, Aoudjit L, Mouawad F, Baldwin C, Nattel S, Takano T.** Nuclear factor of activated T cells mediates RhoA-induced fibronectin upregulation in glomerular podocytes. *Am J Physiol Renal Physiol* 304: F849–F862, 2013. First published February 6, 2013; doi:10.1152/ajprenal.00495.2012.—Glomerulosclerosis is featured by accumulation of the extracellular matrixes in the glomerulus. We showed previously that activation of the small GTPase RhoA in podocytes induces heavy proteinuria and glomerulosclerosis in the mouse. In the current study, we investigated the mechanism by which RhoA stimulates the production of one of the extracellular matrixes, fibronectin, by podocytes, specifically testing the role of nuclear factor of activated T cells (NFAT). Expression of constitutively active RhoA in cultured podocytes activated the fibronectin promoter, upregulated fibronectin protein, and activated NFAT. Expression of constitutively active NFAT in podocytes also activated the fibronectin promoter and upregulated fibronectin protein. RhoA-induced NFAT activation and fibronectin upregulation were both dependent on the calcium/calmodulin pathway and Rho kinase. NFAT activation was also observed in vivo in the rat and mouse models of podocyte injury and proteinuria, and NFAT inhibition ameliorated fibronectin upregulation in the latter. RhoA activation induced a rise of intracellular calcium ion concentration ( $[Ca^{2+}]_i$ ), which was at least in part dependent on the transient receptor potential canonical 6 (TRPC6) cation channel. The results indicate that RhoA activates NFAT by inducing a rise of  $[Ca^{2+}]_i$  in podocytes, which in turn contributes to fibronectin upregulation. This pathway may be responsible for the pathogenesis of certain glomerular diseases such as hypertension-mediated glomerulosclerosis.

fibronectin; glomerulosclerosis; NFAT; podocyte; RhoA

GLOMERULOSCLEROSIS IS A PATHOLOGY featured by accumulation of the extracellular matrixes in the kidney glomerulus and is seen in a wide range of kidney diseases including idiopathic focal segmental glomerulosclerosis (FSGS; Ref. 47), familial FSGS (76), and secondary diseases such as hypertensive nephrosclerosis and diabetic nephropathy (74). In many instances, podocyte injury is postulated to be an underlying cause of glomerulosclerosis; however, how various podocyte injuries ultimately lead to glomerulosclerosis depends on the type and degree of injury and the pathomechanisms are not completely understood (62). A reduced number of podocytes (podocytopenia) following podocyte death was shown to cause glomerulosclerosis in experimental models (74). Indeed, podocytopenia

has been observed in certain human conditions such as diabetic nephropathy and aging, which may explain the development of glomerulosclerosis (74). However, podocytopenia has not been necessarily demonstrated in other conditions and the number of podocytes could be increased in certain forms of FSGS, such as HIV-associated collapsing FSGS (62). Thus mechanisms other than podocytopenia may also contribute to the development of glomerulosclerosis. In this context, overproduction of the extracellular matrixes such as type I collagen and fibronectin by injured/stimulated podocytes could be important. While mesangial cells are well known to produce fibronectin by various stimuli (53, 54), recent studies showed that podocytes can also produce fibronectin, transforming growth factor- $\beta$ , angiotensin II, and high glucose upregulated fibronectin in cultured podocytes (25, 34, 39, 55). Upregulation of the extracellular matrixes was also observed without clear evidence of podocytopenia in adriamycin nephropathy (19) or in a model of diabetic nephropathy (12), and fibronectin staining overlapped, at least partially, with nephrin in the mouse kidney consistent with fibronectin production by podocytes in addition to mesangial cells (70). Furthermore, some investigators propose that podocytes may undergo epithelial-mesenchymal transition when the injury is progressive to escape from apoptotic cell death and that the associated phenotypic changes may contribute to impaired permselectivity (42). Induction of fibronectin and collagen I in injured podocytes was described as part of such a transition (34).

The calcineurin inhibitor cyclosporine A is widely used for the treatment of idiopathic FSGS in addition to glucocorticoids (6). Calcineurin is a serine/threonine phosphatase, which is activated by calmodulin bound to  $Ca^{2+}$  (29). Activated calcineurin, in turn, dephosphorylates the transcription factor nuclear factor of activated T cells (NFAT). Dephosphorylated NFAT translocates from the cytosol to the nucleus and initiates transactivation of the target genes (29). Since NFAT activation is best described in T lymphocytes and many of the known NFAT target genes are proinflammatory, it has been presumed that the effect of cyclosporine A in nephrotic syndrome is via systemic immunosuppression. However, several recent reports suggest that podocytes could be a direct target of calcineurin inhibitors. First, podocyte-specific overexpression of calcineurin was sufficient to cause albuminuria in mice (17). In this study, the authors focused on the role of the non-NFAT target of calcineurin, synaptopodin, to explain the pathomechanisms. In addition to the authors' conclusion, however, the data suggest a possibility that calcineurin activation may induce

Address for reprint requests and other correspondence: T. Takano, Division of Nephrology, McGill Univ. Health Centre, 3775 Univ. St., Rm. 236, Montreal, Quebec H3A2B4, Canada (e-mail: tomoko.takano@mcgill.ca).

detrimental effects on podocytes via its main downstream target, i.e., NFAT. More recently, transient receptor potential canonical 6 (TRPC6) mutations associated with familial FSGS were shown to cause NFAT activation in cultured podocytes, which was inhibited by cyclosporine A (61). In addition, inducible overexpression of a constitutively active mutant of NFAT in podocytes in mice was shown to cause proteinuria and glomerulosclerosis (73), demonstrating that NFAT can play a pathological role directly in podocytes.

RhoA is a prototypical member of the Rho family of small GTPases, which is known as an important mediator of actin cytoskeletal dynamics (5). In cultured mouse podocytes, Rho kinase (downstream kinase of RhoA) was shown to be responsible for mechanical stress-induced cytoskeletal changes (13, 83), suggesting that RhoA activation in podocytes may play a role in podocyte injury in glomerular hyperfiltration/hypertension-induced glomerulosclerosis. We reported previously that inducible expression of a constitutively active (CA) mutant of RhoA (CA-RhoA) in mouse podocytes results in heavy proteinuria and pathology similar to FSGS in humans (82). These results point to a possibility that excessive and/or sustained activation of RhoA may be detrimental to podocyte health and may cause glomerulosclerosis. Consistent with this notion, RhoA activation has been described in podocytes in response to various injurious stimuli such as angiotensin II (26, 28), puromycin aminonucleoside (63), and complement C5b-9 (81). In addition, the Rho-kinase inhibitors (Y27632 and fasudil) were shown to inhibit renal injury and/or albuminuria in various rodent models (21, 33, 53, 63). More recently, it was shown that overexpression of Rho-kinase 1 in podocytes exacerbates, while its deletion ameliorates, podocyte injury in diabetic nephropathy via modulating mitochondrial fission (72).

The current study aimed at studying how RhoA activation in podocytes could lead to extracellular matrix accumulation and glomerulosclerosis. Specifically, we tested the hypothesis that RhoA activation in podocytes induces excess production of the extracellular matrix, fibronectin, via the calcium/calmodulin/calcineurin/NFAT pathway, contributing to the development of glomerulosclerosis.

## MATERIALS AND METHODS

**Materials.** Antibodies were obtained from the following sources: fibronectin (BD Biosciences, San Jose, CA); RhoA, B, and C (Upstate Biotechnology, Lake Placid, NY); HA and NFAT4 (Santa Cruz Biotechnology, Santa Cruz, CA); and TRPC6 (Alomone Labs, Jerusalem, Israel). Antibody for tubulin and all the secondary antibodies were from Jackson ImmunoResearch Laboratories (West Grove, PA). Calpeptin, C3 transferase, and Rho activator II were from Cytoskeleton (Denver, CO). Y27632, VIVIT, BAPTA, W7, FK506, and thapsigargin were from Tocris Bioscience (Minneapolis, MN). 11R-VIVIT (VIVIT for in vivo experiment; Ref. 50) was synthesized at the Sheldon Biotechnology Centre, McGill University. SKF96365 and 2-aminoethoxydiphenyl borate (2-APB) were from Ascent Scientific (Cambridge, MA). Ponasterone A, SB431542 and other chemicals were from Sigma-Aldrich (Mississauga, ON). pGL-F1900 (rat fibronectin promoter-luciferase reporter construct) was a gift from Dr. I. S. Kim (37). pGL3-NFAT-luciferase (containing 3 repeats of the NFAT-binding domain of the human IL-2 promoter), CA-NFAT2 (constitutively active mutant of NFAT2), and HA-NFAT4(3–407)-GFP were obtained from Addgene (Cambridge, MA). pRK5-RhoA(L63)-Myc [constitutively active (CA)-RhoA] and pRK5-RhoA(N19)-Myc [dominant negative (DN)-RhoA] were from Dr. N. Lamarche-Vane (McGill University; Ref. 20).

HA-AT1R was from Dr. S. A. Laporte (McGill University; Ref. 84), and TRPC6 short hairpin (sh)RNAs were from Dr. A. Greka (Harvard Medical School and Massachusetts General Hospital; Ref. 68).

**Cells.** Immortalized mouse podocytes stably expressing rat nephrin were described previously (3). A subclone of mouse podocytes stably expressing the angiotensin receptor AT1R was generated by stably transfecting the AT1R plasmid into immortalized mouse podocytes as described by Attias et al. (3). Mouse podocytes were differentiated by temperature switch for 7–14 days for experiments. A subclone of rat glomerular epithelial cells (GEC) expressing CA-RhoA in a ponasterone A-inducible manner (GEC-RXR-CA-RhoA) was described previously (81).

**Reporter gene assay.** GEC-RXR-CA-RhoA or differentiated mouse podocytes were cultured in a 24-well plate at  $2 \times 10^5$  cells/well. On the following day, 200 ng of the plasmid encoding CA-RhoA or CA-NFAT were cotransfected with 100 ng of FN-luciferase or NFAT-luciferase and 10 ng of pRLTK (Promega, Madison, WI). Inhibitors were added 6 h after the transfection. Cells were harvested 24 h after the transfection, and the luminescence was quantified using Dual Luciferase Assay System (Promega).

**Immunofluorescence staining.** Immunofluorescence staining was carried out as described previously (82). In brief, GEC-RXR-CA-RhoA or differentiated mouse podocytes were cultured on glass coverslips and were placed in 12-well plates. On the following day, cells were transfected with plasmids (400 ng/well). After 24 h, cells were fixed with 3.2% paraformaldehyde and permeabilized with 0.5% Triton X-100. Incubations with the first and second antibodies were carried out at 4°C overnight and at 22°C for 60 min, respectively. Staining of mouse kidneys for fibronectin and podocalyxin was described previously (82). Images for NFAT4 nuclear translocation were captured on a LSM 780 Laser Scanning Confocal Microscope (Zeiss, Germany). All the other images were captured with an AxioObserver-100 microscope (Zeiss).

**Cell fractionation.** Separation of the nuclear and cytosolic cellular fractions was carried out as described previously (59) with minor modifications. Briefly, GEC-RXR-CA-RhoA were transiently transfected with HA-NFAT4(3–407)-GFP and stimulated with calpeptin (Rho activator, 100 µg/ml) in the presence or absence of Y27632 (10 µM) or with ionomycin (2 µM) for 45 min at 37°C. The nuclear and cytosolic fractions were separated as by Richardson et al. (59) and localization of NFAT4 was studied by immunoblotting for HA.

**Immunoblotting.** Immunoblotting was carried out as described previously (66). In brief, cells were lysed with buffer containing 10 mM sodium pyrophosphate, 25 mM NaF, 2 mM Na<sub>3</sub>VO<sub>4</sub>, 1% Triton X-100, 125 mM NaCl, 10 mM Tris, 1 mM EDTA, 1 mM EGTA, and a protease inhibitor cocktail (Roche Diagnostics, Basel, Switzerland), pH 7.4. Protein concentration was determined, and samples containing equal amounts of protein were separated by 4–15% (wt/vol) gradient (fibronectin) or 7.5% SDS-PAGE (TRPC6) and transferred to polyvinylidene difluoride membranes (Bio-Rad Laboratories, Hercules, CA). Blots were incubated with primary antibodies overnight and subsequently with peroxidase-labeled secondary antibodies. Proteins were visualized using enhanced chemiluminescence, and signal intensity was determined with ImageJ.

**RT-PCR.** Total RNA was extracted and DNase-treated. Synthesis of cDNA was performed with 1 µg of total RNA using the Reverse Transcription Reagents Kit from Qiagen (Valencia, CA). Primers used are shown in Table 1. Primers for fibronectin were purchased from Qiagen (no. QT00135758).

**Quantification of fibronectin by ELISA.** Rat fibronectin ELISA was performed following the manufacturer's instructions (Biorbyt, Cambridge, UK) using 100 µl of cell lysates from GEC-RXR-CA-RhoA stimulated with ponasterone A.

**shRNA-mediated gene silencing.** Gene silencing was performed as described previously (68). Briefly, differentiated mouse podocytes were transduced with lentivirus containing shRNAs or control shRNAs. Virus

Table 1. PCR primers

	Forward Primer	Reverse Primer
Rat NFAT1	CGCGTGTGGCCCTTGTGTTC	AGGGGGACTCGGCCAGCATT
Rat NFAT2	AGAGGCTCCGAAGTGGGCGA	GGCAAGGCGGAGTGTGCTGT
Rat NFAT3	GCCCATCGAGTGTCCCAGC	AGGCCTAAAGGGGGCCGGAG
Rat NFAT4	GGGCCACGCCGATGACTACTG	TCAGCACTGGAGTGCCTCG
Mouse NFAT1a	CAGGGCTCCACCTCCGACA	GGTCCAGCAGACAGGGAGCCA
Mouse NFAT1b	GGCCCCGGGACTCTATACG	AGCGGGGATGCTGTGCTCCT
Mouse NFAT1c	ACCATGGCCCCCTGCCAACA	GCTGGCCGAGGATGTGTGTCGGA
Mouse NFAT2	GTGGCAGCCATCAAGCCCT	CCCCGTGATCCGGTGGACCT
Mouse NFAT3	CCGACCTCGCTAGAGGACACTCC	TGTCCCCCAATCCGGGCCTT
Mouse NFAT4	CCTCAGCCCTGCACCGTTCC	CCACTGGGCTGTGGGATGTGC
AT1a receptor	GCATCATCTTTGTGGTGGG	ATCAGCACATCCAGGAATG

NFAT, nuclear factor of activated T cells; AT1a receptor, angiotensin II type 1a receptor.

containing medium was replaced after 18 h. Cells were used for calcium measurement 72 h after start of transduction.

**Measurement of the intracellular calcium ion concentration.** Measurement of the intracellular calcium ion concentration ( $[Ca^{2+}]_i$ ) was carried out as described previously (49). Briefly, cells were plated on glass bottom microwell dishes (MatTek, Ashland, MA). Cells were incubated with fluo-4 (5  $\mu$ M) at room temperature for 5 min and washed three times in RPMI 1640 without phenol red. The calcium fluorescence (excitation: 488 nm and emission: between 500–650 nm) was imaged by a confocal microscope (Olympus IX-81). Calcium images were recorded every 10 min.

**EMSA.** Glomeruli from rats and mice were prepared by differential sieving as described previously (3, 82). Nuclear extracts of the glomerulus were prepared following the protocol as described previ-

ously (67). EMSA was performed using the NFAT EMSA kit (cat. no. AY1027P; Panomics, Fremont, CA), which uses the NFAT-binding sequence from the interleukin-2 gene as a probe (51). Specificity of the shifted band was confirmed by adding excess cold probe. In some experiments, anti-NFAT4 antibody (sc-8405x; Santa Cruz) was added for supershift.

**Animals.** Mice with podocyte-specific, doxycycline-inducible CA-RhoA were described previously (82). For the NFAT inhibition experiment, mice were treated with doxycycline (4 mg/ml in drinking water) for 1 wk with or without the NFAT inhibitor 11R-VIVIT (10 mg/kg ip in PBS) for the last 5 days. Puromycin aminonucleoside nephrosis was induced by a single intravenous injection of puromycin aminonucleoside (100 mg/kg) in male Sprague-Dawley rats (150–175 g) as described previously (1).

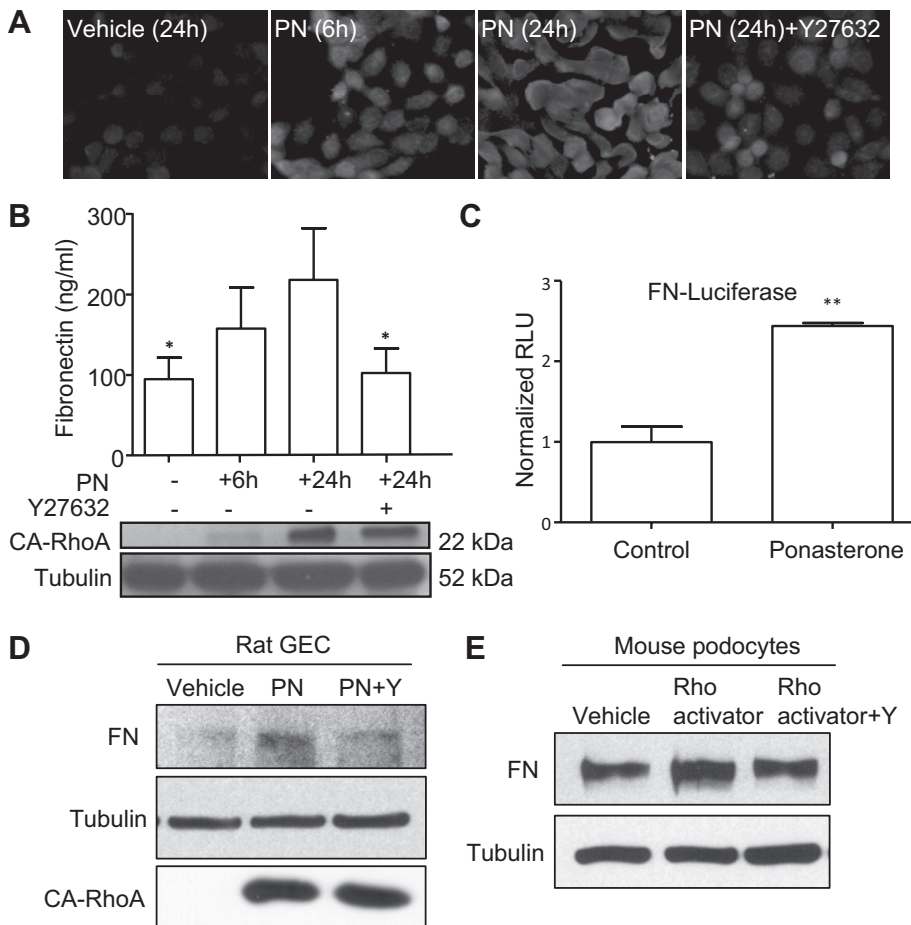


Fig. 1. Fibronectin is upregulated by RhoA activation in podocytes. *A–D*: rat visceral glomerular epithelial cells (GEC), which express a constitutively active (CA) mutant of RhoA (CA-RhoA) in a ponasterone A-inducible manner (GEC-RXR-CA-RhoA) were stimulated with ponasterone A (PN; 1  $\mu$ M) or vehicle. *A*: cells were immunostained for fibronectin. Fibronectin was upregulated in a time-dependent manner, which was inhibited by Y27632 (Rho-kinase inhibitor, 10  $\mu$ M). Magnification:  $\times 400$ . *B*: cell lysates were analyzed for fibronectin protein by ELISA (top).  $*P < 0.05$  vs. ponasterone 24 h;  $n = 4$ . *Bottom*: induction of CA-RhoA by immunoblotting (with tubulin as a loading control). *C*: fibronectin promoter connected to luciferase (FN-luciferase) was transfected into GEC-RXR-CA-RhoA. After 24 h of ponasterone A stimulation, cell lysates were analyzed for luciferase activity.  $***P < 0.001$  vs. control;  $n = 4$ . *D*: cells were stimulated for 24 h with ponasterone A (0.5  $\mu$ M) with or without Y27632 (Y, 10  $\mu$ M) and cell lysates were immunoblotted for fibronectin, RhoA, and tubulin (loading control). *E*: differentiated mouse podocytes were stimulated for 24 h with the Rho activator II (0.2  $\mu$ g/ml) with or without Y27632 and cell lysates were immunoblotted for fibronectin and tubulin (loading control). RLU, relative light units.

**Statistical analysis.** Data are expressed as means ± SE. Student's *t*-test was used to determine significant differences between two groups. One-way ANOVA was used to compare multiple groups using the Newman-Keuls test for post hoc analysis. *P* < 0.05 was considered significant.

**RESULTS**

**RhoA upregulates fibronectin in podocytes.** We reported previously that induction of CA-RhoA in mouse podocytes results in FSGS-like pathology, which was accompanied by an upregulation of fibronectin mRNA and protein levels in the glomerulus (82). We first confirmed if RhoA activation leads to fibronectin upregulation in cultured podocytes. We utilized a subclone of rat GEC, which express CA-RhoA in a ponasterone A-inducible manner (GEC-RXR-CA-RhoA) (81). Ponasterone A is an insect hormone and has no known impacts on

mammalian cells (81). Thus the system allows evaluating the impact of RhoA activation on the cell. We established that a low dose of ponasterone A (1 μM) allows a mild induction of CA-RhoA without causing cell death (82). When the cells were treated with a low dose of ponasterone A, immunostaining for fibronectin was increased starting at 3 h (Fig. 1A). The upregulation was inhibited by an inhibitor of Rho kinase (Y27632), which acts downstream of activated RhoA (5). Similar results were confirmed by ELISA and immunoblotting (Fig. 1, B and D). In addition, when the fibronectin promoter-reporter construct was transfected into the cells and treated with ponasterone A for 24 h, luciferase activity was significantly augmented, compared with vehicle-treated cells (Fig. 1C). Thus induction of CA-RhoA in rat GEC activates the fibronectin gene, leading to protein upregulation. We also confirmed that RhoA activation leads to

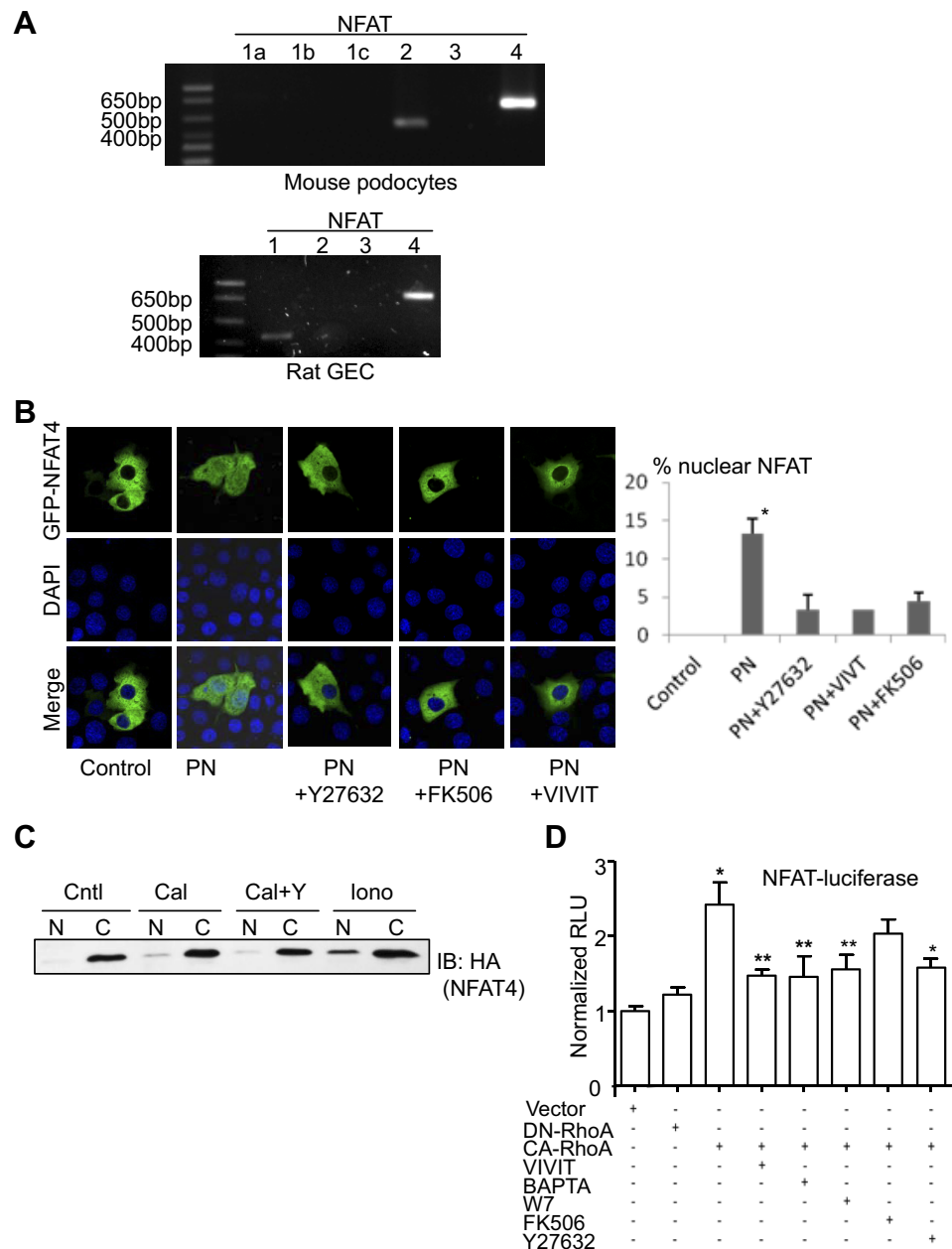


Fig. 2. RhoA activates nuclear factor of activated T cells (NFAT) in podocytes. **A:** NFAT isoforms were amplified from the total cell RNA by RT-PCR. NFAT4 was predominantly expressed both in rat GEC and mouse podocytes. **B:** nuclear translocation of NFAT was studied by confocal microscopy. GFP-NFAT4 transfected rat GEC was localized exclusively in the cytosol, while induction of CA-RhoA by ponasterone A (1 μM, 24 h) induced nuclear translocation, which was blocked by Y27632 (Rho-kinase inhibitor, 10 μM), FK506 (calcineurin inhibitor, 5 μM), and VIVIT (NFAT inhibitor, 5 μM). Magnification: ×630. **Right:** percentage of GFP-NFAT4-transfected cells, which showed nuclear staining; *n* = 90 cells from 3 independent experiments. **IB,** immunoblot. \**P* < 0.05 vs. all the others. **C:** rat GEC were transiently transfected with HA-NFAT4 and stimulated with calpeptin (Cal; 100 μg/ml) in the presence or absence of Y27632 (Y; 10 μM) or with ionomycin (Iono; 2 μM) for 45 min. Nuclear (N) and cytosolic (C) cellular fractions were studied by immunoblotting for HA. **D:** the reporter construct NFAT-luciferase was transfected into mouse podocytes with CA-RhoA, inactive mutant of RhoA (DN-RhoA), or empty vector. Cell lysates were analyzed for luciferase activity after 24 h. VIVIT (5 μM), BAPTA-AM (intracellular calcium ion chelator, 10 μM), W7 (calmodulin inhibitor, 1 μM), FK506 (5 μM), or Y27632 (10 μM) was added overnight before cell lysis. \**P* < 0.01 CA-RhoA vs. vehicle; \*\**P* < 0.01 CA-RhoA vs. inhibitors; *n* = 9.

fibronectin protein upregulation in cultured mouse podocytes (Fig. 1E).

**RhoA activates NFAT in podocytes.** We next studied how RhoA transactivates the fibronectin gene. Since a significant percentage of patients with FSGS respond to treatment with a calcineurin inhibitor (6), we hypothesized a potential role of the calcineurin-NFAT pathway. We first studied which of the four known NFAT isoforms are expressed in the cultured podocytes by RT-PCR. In rat GEC and mouse podocytes used in the current study, we identified predominant expression of NFAT4 (NFATc3) mRNA, consistent with the previous report (61) (Fig. 2A). It is known that NFAT, when dephosphorylated by calcineurin, translocates from the cytosol to the nucleus (57). When GFP-NFAT4 was transfected in GEC-RXR-CA-RhoA, it localized exclusively in the cytosol, consistent with its phosphorylated/inactive state at the baseline (Fig. 2B). When cells were stimulated with ponasterone A to induce CA-RhoA expression, ~13% of the cells showed clear nuclear localization of GFP-NFAT4, while no nuclear localization was observed in control (vehicle-treated) cells (Fig. 2B). RhoA-induced nuclear translocation was abolished by the NFAT inhibitor (VIVIT), calcineurin inhibitor (FK506), and Rho-kinase inhibitor (Y27632; Fig. 2B). We also confirmed NFAT4 nuclear translocation biochemically; when rat GEC was transfected with HA-NFAT4 and stimulated with calpeptin (Rho activator), NFAT4 in the nuclear fraction increased, albeit the effect of calpeptin was weaker than the well-established NFAT activator ionomycin (Fig. 2C).

Next, the NFAT-responsive reporter was tested in mouse podocytes. CA-RhoA activated the NFAT reporter significantly, which was inhibited by the NFAT inhibitor (VIVIT), intracellular calcium chelator (BAPTA), calmodulin inhibitor (W7), and the Rho-kinase inhibitor (Y27632; Fig. 2D). The calcineurin inhibitor FK506 also inhibited the NFAT reporter activation, but the inhi-

bition was partial (see DISCUSSION). The inactive mutant of RhoA did not activate the NFAT promoter (Fig. 2D). CA-RhoA-mediated NFAT-reporter activation was also confirmed in rat GEC (not shown). Taken together, the results indicate that RhoA activates NFAT in a Rho-kinase- and calcium/calmodulin/cal-cineurin/NFAT-dependent manner in podocytes.

**NFAT upregulates fibronectin in podocytes.** We next studied if NFAT activation itself can induce fibronectin upregulation in podocytes. First, the fibronectin promoter-reporter was tested in mouse podocytes. CA-NFAT induced a significant activation of the fibronectin promoter, which was synergistically augmented further by the protein kinase C activator phorbol 12-myristate 13-acetate, similar to many other genes such as interleukin-2 (44) (Fig. 3A). We next studied if the transcriptional activation of fibronectin also results in protein upregulation. When wild-type NFAT (GFP-tagged) was transfected into mouse podocytes, it localized in the cytosol, consistent with its inactive state (Fig. 3B). Immunostaining for fibronectin was minimal (Fig. 3B) and was not different from cells transfected with GFP alone (not shown). In contrast, CA-NFAT localized predominantly in the nucleus as expected and the expression of fibronectin in the transfected cell was markedly increased (Fig. 3B). Thus NFAT activation was sufficient to transactivate the fibronectin gene and upregulate fibronectin protein in podocytes.

**RhoA-induced fibronectin upregulation is dependent on NFAT activation.** The results, thus far, clearly demonstrate that RhoA activates NFAT and upregulates fibronectin. Furthermore, fibronectin upregulation was shown to be NFAT dependent, which led us to ask if NFAT mediates RhoA-induced fibronectin upregulation in podocytes. The fibronectin promoter-reporter was activated by CA-RhoA, but not by the inactive mutant of RhoA, in mouse podocytes (Fig. 4A), consistent with the results in rat GEC as shown in Fig. 1C. RhoA-induced

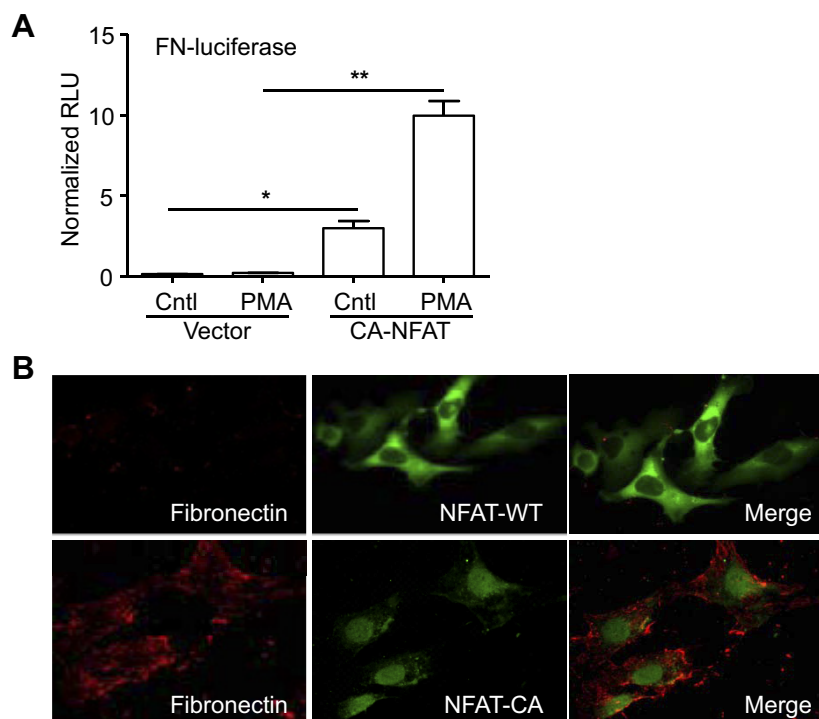


Fig. 3. NFAT up-regulates fibronectin in podocytes. **A:** FN-luciferase was transfected into podocytes with a constitutively active mutant of NFAT (CA-NFAT) or empty vector. Cell lysates were analyzed for luciferase activity after 24 h. Phorbol 12-myristate 13-acetate (PMA; 5 ng/ml) was added overnight before cell lysis. \* $P < 0.01$  CA-NFAT vs. vehicle; \*\* $P < 0.01$  PMA vs. no PMA;  $n = 6$ . **B:** mouse podocytes were transfected with wild-type NFAT (*top*, GFP-tagged) or CA-NFAT (*bottom*, HA-tagged) and immunostained for fibronectin or HA. Wild-type NFAT localized in the cytosol while CA-NFAT localized in the nucleus. CA-NFAT upregulated fibronectin in the transfected cell. Magnification:  $\times 630$ .

fibronectin gene transactivation was inhibited by VIVIT, BAPTA, W7, and Y27632. FK506 also inhibited the fibronectin reporter activation but the inhibition was incomplete, similar to RhoA-induced NFAT activation as shown in Fig. 2C (see DISCUSSION). We also studied the inhibitory profile of RhoA-induced fibronectin protein in rat GEC. Similar to the

results of the reporter gene assay, RhoA-induced fibronectin upregulation was inhibited by VIVIT, BAPTA, W7, and Y27632 (Fig. 4B). Transforming growth factor- $\beta$  (TGF- $\beta$ ) is a well-known potent transactivator of fibronectin (54). However, the TGF- $\beta$  receptor I inhibitor, SB431542 (10  $\mu$ M) did not inhibit RhoA-induced fibronectin gene transactivation, indicating that the effect of RhoA on fibronectin is independent of TGF- $\beta$  (Fig. 4C). These results suggest that RhoA transactivates the fibronectin gene via Rho-kinase and the calcium/calmodulin/NFAT pathway, but not via TGF- $\beta$ , thereby contributing to protein upregulation.

NFAT is activated in the models of podocyte injury and contributes to fibronectin upregulation. The role of NFAT in podocyte-mediated glomerulosclerosis has been proposed by several groups (48, 61, 73). However, direct evidence for NFAT activation in proteinuric glomerular disease/model in vivo is sparse. We next studied NFAT activation in vivo. First, podocyte-specific CA-RhoA expression was induced in mice and glomerular nuclear extracts were analyzed by EMSA using an NFAT-binding probe. Glomeruli from control mice showed a minimal mobility shift of the NFAT probe, which was markedly increased when mice were induced with doxycycline for 2 days, consistent with the nuclear translocation of NFAT (Fig. 5A). The shifted band was abolished by addition of excess cold probe demonstrating the specificity (Fig. 5A). The expression of CA-RhoA is limited to podocytes in this model; thus it is reasonable to assume that the nuclear translocation of NFAT takes place in podocytes. Since the predominant NFAT isoform in cultured podocytes was NFAT4 (Fig. 2A), we added NFAT4 antibody to the reaction to test its ability to supershift the band. The band intensity became markedly weaker with the addition of NFAT4 antibody, suggesting that the major NFAT, which caused the mobility shift of the NFAT probe, was NFAT4. However, we were not able to identify the supershifted band, which is expected to be seen at the higher part of the gel. This could be because of an intense and broad non-specific band at the top of the gel (not shown).

Next, we studied glomeruli from rats with PAN. Nuclear extracts from control rat glomeruli showed a minimal mobility shift (Fig. 5B), similar to control mice (Fig. 5A). In contrast, glomeruli from rats 4 days after disease induction showed a distinct mobility shift of the NFAT probe (Fig. 5B). The shifted band was abolished by excess cold probe and anti-NFAT4 antibody, similar to CA-RhoA expressing mice (Fig. 5B). Since podocyte is the main site of injury in this model, NFAT activation is likely to be taking place in podocytes although NFAT activation in other cell types cannot be excluded.

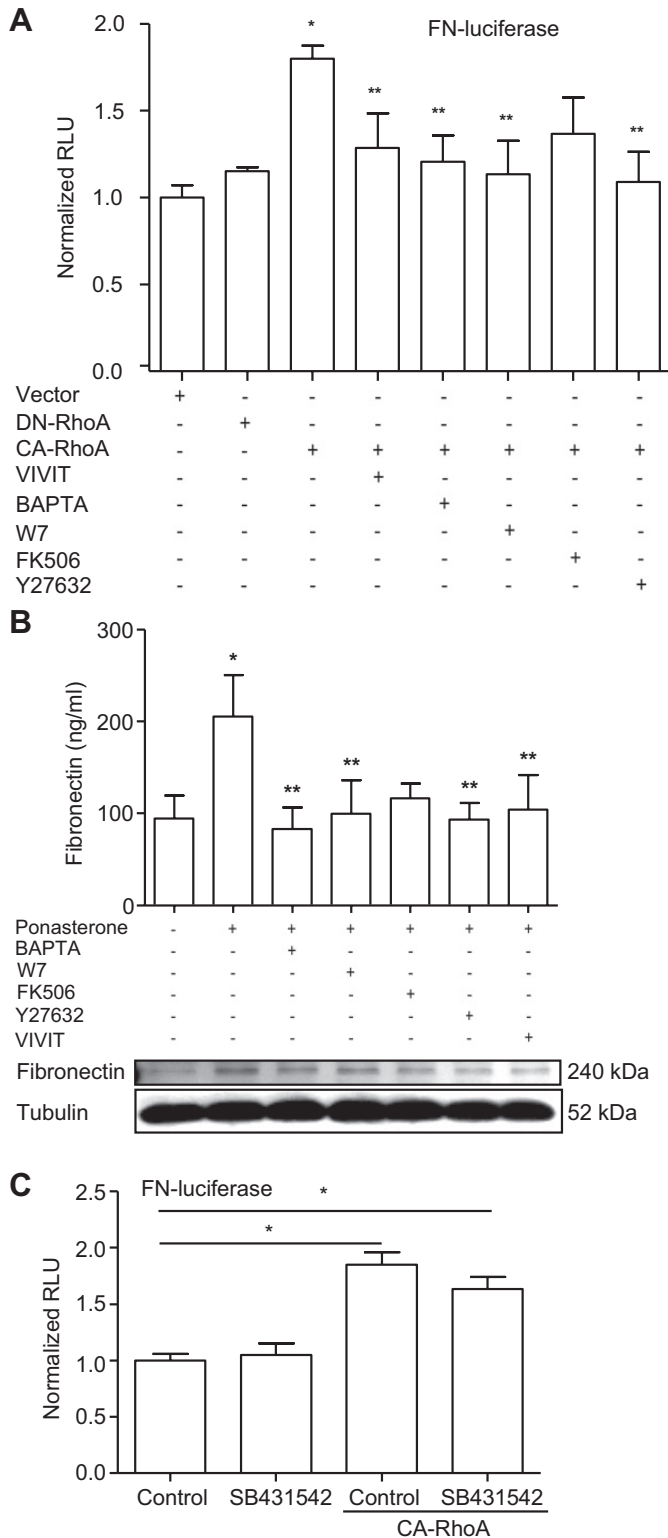


Fig. 4. RhoA-induced fibronectin upregulation is dependent on NFAT. **A:** FN-luciferase was transfected into mouse podocytes with CA-RhoA, inactive mutant of RhoA (DN-RhoA), or empty vector. Cell lysates were analyzed for luciferase activity after 24 h. Inhibitors were added as in Fig. 2. \* $P < 0.01$  CA-RhoA vs. vehicle; \*\* $P < 0.01$  CA-RhoA vs. inhibitors;  $n = 9$ . **B:** GEC-RXR-CA-RhoA was induced with ponasterone A as in Fig. 1B for 24 h with the indicated inhibitors or vehicle and cell lysates were analyzed by ELISA (top) or immunoblotting. \* $P < 0.05$  CA-RhoA vs. control; \*\* $P < 0.05$  CA-RhoA vs. inhibitors;  $n = 4$ . Concentrations of the inhibitors are the same as in Fig. 2. **C:** FN-luciferase was transfected into mouse podocytes with CA-RhoA. SB431542 (TGF- $\beta$  receptor 1 inhibitor, 10  $\mu$ M) was added overnight. After 24 h of transfection, cell lysates were analyzed for luciferase activity. \* $P < 0.01$ ;  $n = 6$ .

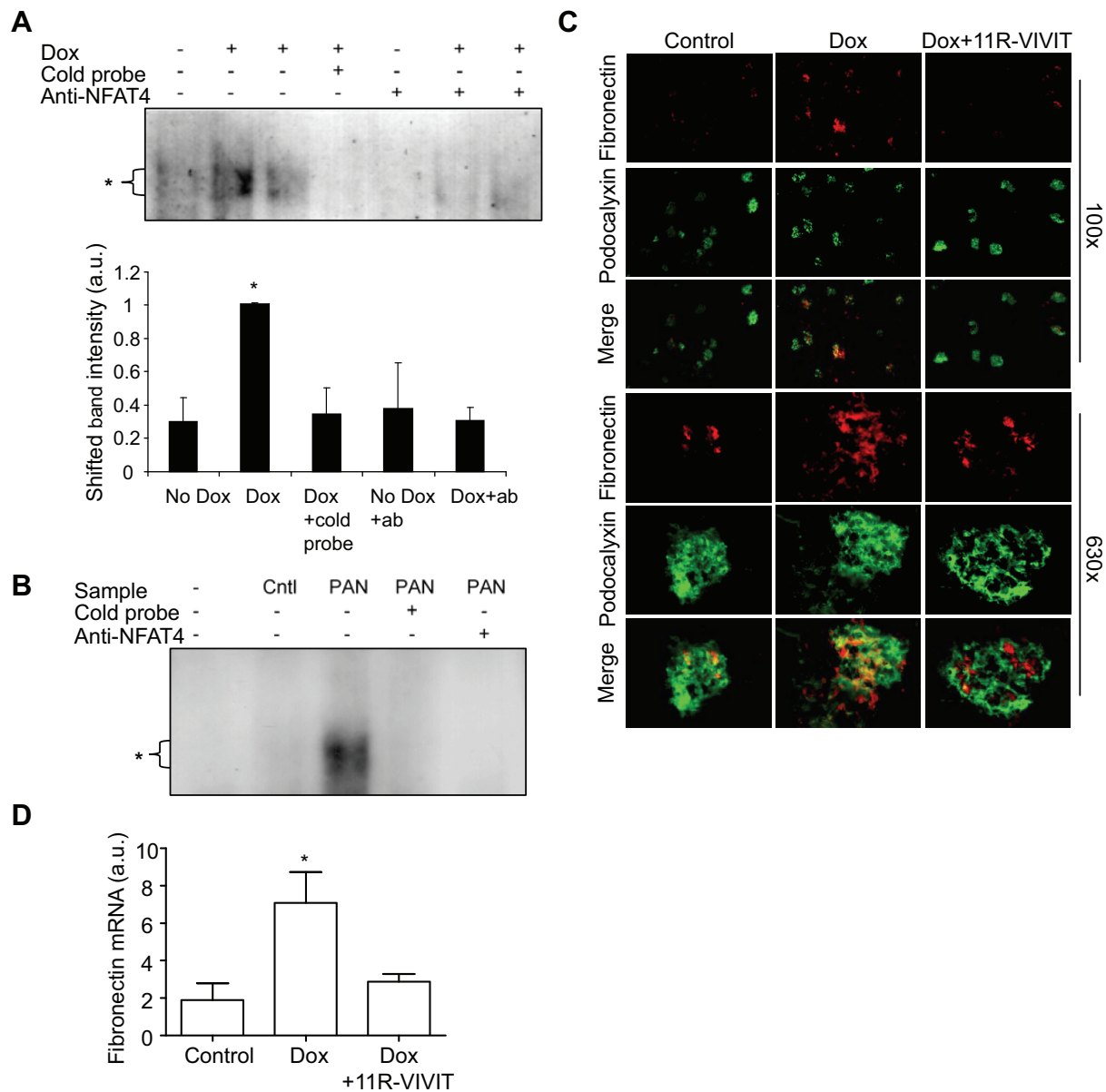


Fig. 5. NFAT is activated in the rat and mouse model of podocyte injury and proteinuria and contributes to fibronectin upregulation. *A*: podocyte-specific expression of CA-RhoA was induced by doxycycline (Dox) in mouse for 2 days. Control mice were treated with vehicle. *B*: puromycin aminonucleoside nephrosis (PAN) was induced by a single intravenous injection of puromycin aminonucleoside in rats. Control rats were injected with saline. Animals were killed on *day 4*. Nuclear extracts from the glomerulus were subjected to EMSA using an NFAT-specific probe (see MATERIALS AND METHODS). NFAT in the glomerular nuclear extracts was minimal in control animals but markedly increased in Dox-treated mice (*A*) and in PAN rats (*B*). The shifted bands (\*) were abolished by adding excess cold probe, demonstrating the specificity. Addition of anti-NFAT4 antibody also markedly reduced the intensity of the shifted band, suggesting supershift. However, we were not able to identify the supershifted bands, possibly because of the intense nonspecific bands at the top of the gel (not shown). *A*, *bottom*: densitometric analysis of the shifted band. \* $P < 0.05$  vs. all the others;  $n = 4-5$  mice each per group. *C* and *D*: podocyte-specific expression of CA-RhoA was induced by doxycycline in mouse for 1 wk, with or without the NFAT inhibitor, 11R-VIVIT. Control mice were treated with vehicle alone. *C*: kidney sections were immunostained for fibronectin and podocalyxin. Dox-treated mice (*middle*) showed increased expression of fibronectin in glomeruli, compared with control (*left*), or mice treated with Dox plus 11R-VIVIT (*right*). Magnification:  $\times 100$  (*top*) and  $\times 630$  (*bottom*). *D*: glomerular lysates were analyzed by qPCR for fibronectin mRNA expression.  $P < 0.05$ , Dox vs. control;  $n = 4-6$  mice in each group.

Finally, we tested the effect of a pharmacological inhibitor of NFAT on fibronectin upregulation *in vivo*. When CA-RhoA was induced in podocytes in mice, glomerular fibronectin mRNA was upregulated (Fig. 5, *C* and *D*), consistent with our previous report (82). Immunostaining of fibronectin in doxycycline-treated glomeruli overlapped, at least partially, with podocalyxin, suggesting that fibronectin upregulation occurred in podocytes (Fig. 5*C*). The upregulation was inhibited by

11R-VIVIT (Fig. 5, *C* and *D*). Proteinuria, as quantified by the urine albumin-to-creatinine ratio, was not affected by 11R-VIVIT (not shown). Together, the results indicate that NFAT is activated in certain models of podocyte injury and contributes to fibronectin upregulation.

*Activation of RhoA increases the intracellular calcium.* We next asked how RhoA activates NFAT in podocytes. NFAT activation is known to be triggered by a rise of the  $[Ca^{2+}]_i$  (11).

Therefore, we studied the effect of RhoA activation on  $[Ca^{2+}]_i$ . First, we induced the expression of CA-RhoA in rat GEC and quantified  $[Ca^{2+}]_i$  using a fluorescence dye, fluo-4. Fluo-4 loaded in the cell binds to free  $Ca^{2+}$  and emits fluorescence when excited by the 488 nm laser. Unlike the ratio-metric dye, fura-2, fluo-4 does not allow the quantification of the absolute  $[Ca^{2+}]_i$  values but can be used to monitor relative changes of the  $[Ca^{2+}]_i$ . When mouse podocytes loaded with fluo-4 were stimulated with a RhoA activator, calpeptin, a gradual and steady increase of  $[Ca^{2+}]_i$  was observed over the period of 40 min (Fig. 6A). The RhoA inhibitor C3 transferase and the Rho-kinase inhibitor Y27632 abrogated the calpeptin-induced  $[Ca^{2+}]_i$  rise (Fig. 6B), indicating that calpeptin increases  $[Ca^{2+}]_i$  via RhoA and Rho kinase. A similar slow rise of  $[Ca^{2+}]_i$  was also observed in pulmonary capillary endothelial cells via the transient receptor potential channel TRPV4 (78) and in HeLa-S3 and U2-OS cells stimulated with cisplatin (65). Furthermore, when GEC-RXR-CA-RhoA were stimulated with ponasterone A to induce CA-RhoA activation,  $[Ca^{2+}]_i$  became significantly higher, compared with vehicle-treated cells, confirming that RhoA activation leads to a rise of  $[Ca^{2+}]_i$  (Fig. 6C).

A rise of  $[Ca^{2+}]_i$  could be secondary to extracellular-to-intracellular  $Ca^{2+}$  influx or to the release of  $Ca^{2+}$  from the intracellular stores (22). When  $[Ca^{2+}]_i$  measurement was carried out in a buffer containing zero  $Ca^{2+}$ , calpeptin-induced  $[Ca^{2+}]_i$  rise was abolished, suggesting that the calpeptin-induced rise of  $[Ca^{2+}]_i$  is dependent on the extracellular

calcium (Fig. 7A). Podocytes are known to express TRPC cation channels (22). In particular, mutations of TRPC6 are known to be associated with the pathogenesis of familial FSGS (58, 77). We next stimulated the cells with calpeptin in the presence of 2-APB (30  $\mu$ M) or SKF96365 (25  $\mu$ M), both of which are known to block the TRPC channels (27, 30). The calpeptin-induced rise of  $[Ca^{2+}]_i$  was significantly inhibited by the two inhibitors (Fig. 7A), suggesting that calpeptin induces  $Ca^{2+}$  influx via TRPC channels. When TRPC6 was knocked down by shRNA, the calpeptin-induced rise of  $[Ca^{2+}]_i$  was significantly reduced, further supporting the contribution of TRPC6 (Fig. 7B). Furthermore, in the presence of thapsigargin (100 nM), which inhibits the  $Ca^{2+}$ -ATPase and depletes the intracellular  $Ca^{2+}$  store (60), the calpeptin-induced  $[Ca^{2+}]_i$  rise was inhibited significantly (Fig. 7A). Thus RhoA activation induces a rise of  $[Ca^{2+}]_i$ , which is dependent on both the intracellular  $Ca^{2+}$  stores and the extracellular  $Ca^{2+}$ . The influx of the latter appears to be, at least in part, dependent on the TRPC channels. Whether the calcium influx induced calcium release from the stores (14) and/or the calcium release activated the store-operated calcium channels (52) could not be determined from the current studies.

We also studied the impact of RhoA activation on the expression level of TRPC6 in rat GEC. After 24 h of CA-RhoA induction, TRPC6 expression was upregulated, which was inhibited by the Rho-kinase inhibitor (Fig. 7C). Thus RhoA

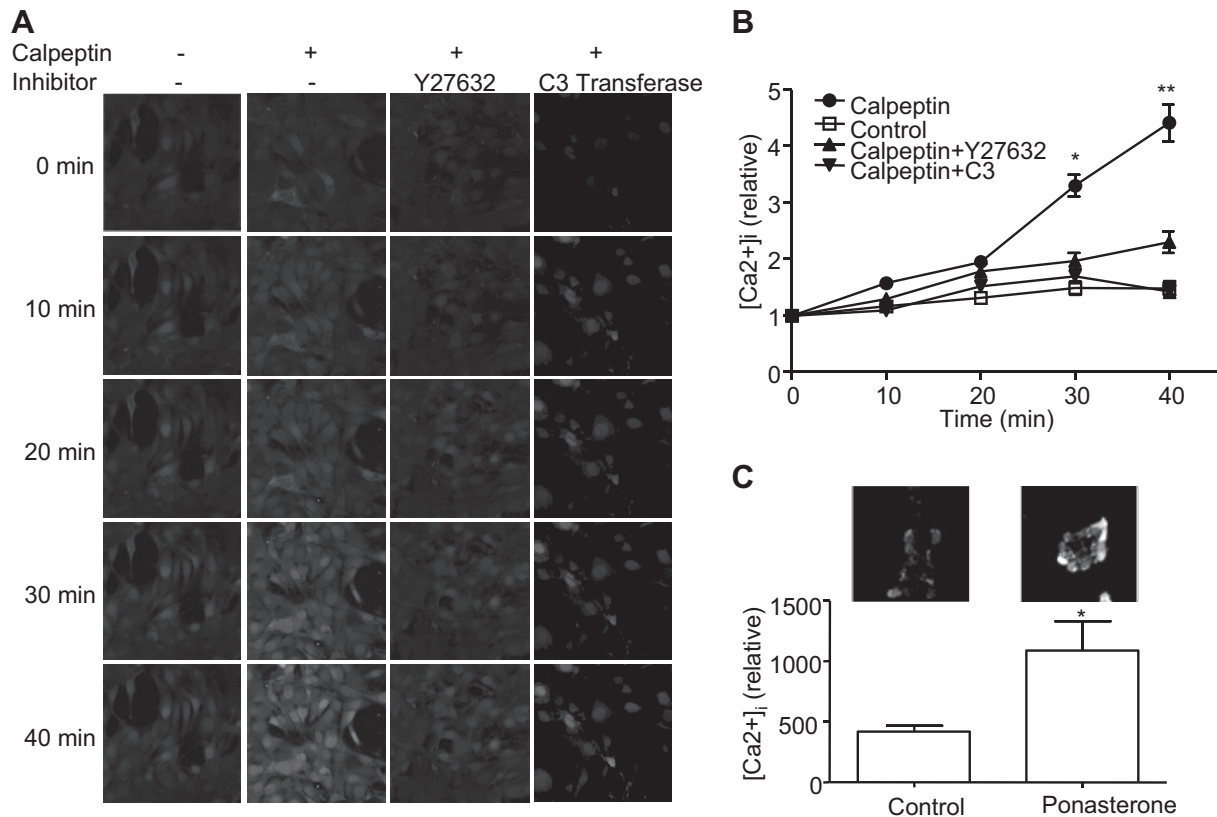


Fig. 6. Activation of RhoA increases intracellular calcium in podocytes. A: mouse podocytes were stimulated with calpeptin (Rho activator, 100  $\mu$ g/ml) for the indicated times and the intracellular calcium ion concentration ( $[Ca^{2+}]_i$ ) was measured with fluo-4. Y27632 (Rho-kinase inhibitor, 10  $\mu$ M) and the C3 transferase (Rho inhibitor, 1  $\mu$ g/ml), were added 16 h and 6 h before the calcium measurement, respectively. Magnification:  $\times 400$ . B:  $[Ca^{2+}]_i$  was quantified as the fluorescence intensity of B and normalized to time zero. \* $P < 0.05$ , \*\* $P < 0.001$  vs. control;  $n = 12-20$  cells. C: GEC-RXR-CA-RhoA were stimulated with ponasterone A (1  $\mu$ M) for 16 h to induce the expression of CA-RhoA.  $[Ca^{2+}]_i$  was measured using with fluo-4. CA-RhoA-expressing cells showed a significantly higher  $[Ca^{2+}]_i$  compared with vehicle-treated cells. \* $P < 0.05$ ;  $n = 8-10$  cells.



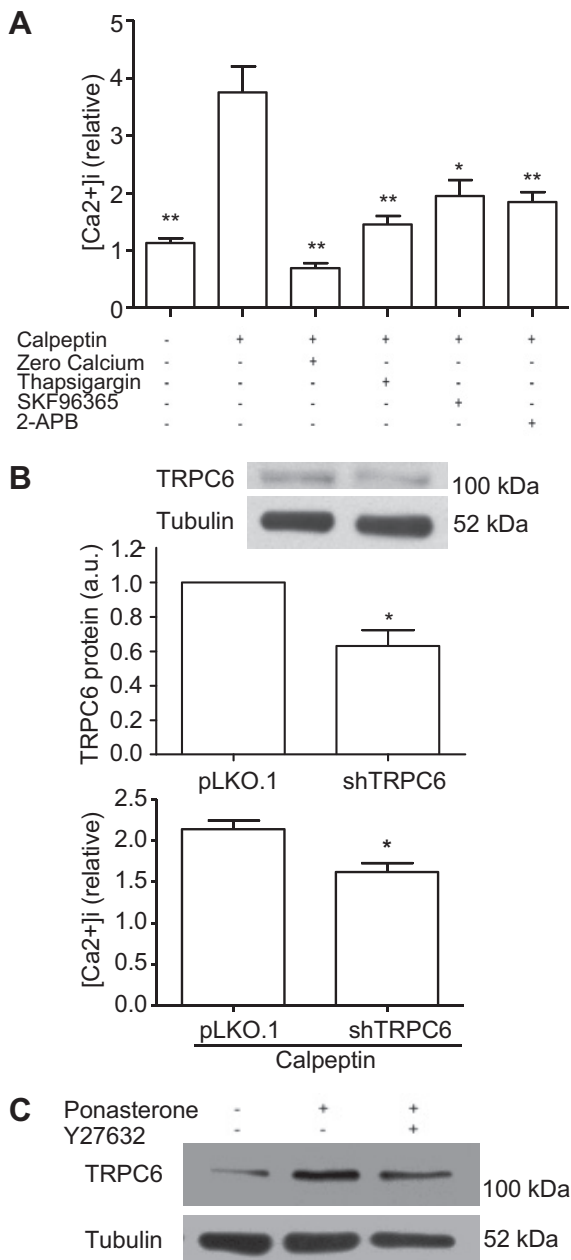


Fig. 7. RhoA induces  $\text{Ca}^{2+}$  influx via TRPC channels in podocytes. **A**: mouse podocytes were stimulated with calpeptin as in Fig. 6 for 40 min in the presence of calcium-free buffer, thapsigargin (100 nM), SKF-96365 (25  $\mu\text{M}$ ), or 2-aminoethoxydiphenyl borate (2-APB; 30  $\mu\text{M}$ ). For each experiment, fluorescence intensity from 10–20 cells were averaged and normalized to the baseline. The results are the means  $\pm$  SE from 3 independent experiments ( $*P < 0.05$ ,  $**P < 0.01$  vs. calpeptin + vehicle). **B**: mouse podocytes were transduced with lentivirus containing TRPC6 shRNAs or vector alone (control) as described in MATERIALS AND METHODS. Forty-eight hours after the transduction, cells were lysed or serum starved overnight. Cell lysates were analyzed for TRPC6 protein by immunoblotting (top) and quantified by densitometry (middle, normalized to tubulin). Serum starved cells were stimulated with calpeptin and  $[\text{Ca}^{2+}]_i$  was measured (bottom).  $*P < 0.05$  control vs. shRNA;  $n = 3$  (immunoblot), 3 independent experiments with 10–20 cells each ( $[\text{Ca}^{2+}]_i$  measurement). **C**: GEC-RXR-CA-RhoA were treated with ponasterone A (1  $\mu\text{M}$ , 24 h) with or without Y27632 (10  $\mu\text{M}$ ). Cell lysates were immunoblotted for TRPC6 and tubulin (loading control).

may also modulate  $[\text{Ca}^{2+}]_i$  by regulating the expression level of TRPC6.

*Angiotensin II-induced fibronectin upregulation is dependent on NFAT but not on Rho kinase.* Angiotensin II was shown to act on podocytes and is likely to be relevant to the pathogenesis of diabetic nephropathy or hypertensive nephrosclerosis (28, 38, 85). It has been reported that angiotensin II stimulates fibronectin production by podocytes (25). Since angiotensin II is known to increase the intracellular calcium (23) and also to activate RhoA and NFAT (48, 68), we next studied if RhoA and/or the calcium/calmodulin/NFAT pathway mediate angiotensin II-induced fibronectin production. In cultured mouse podocytes used in the current study, the angiotensin II receptors AT1a, AT1b, and AT2 were expressed at the mRNA level but the response to angiotensin II was weak (not shown). Therefore, we developed a line of mouse podocyte, which stably express the AT1a receptor (MP-AT1R; Fig. 8A). When these cells were stimulated with angiotensin II, fibronectin protein was upregulated, consistent with the previous report (25) (Fig. 8B). In MP-AT1R, angiotensin II activated the fibronectin promoter, which was inhibited by BAPTA, W7, FK506, and VIVIT (Fig. 8C). In contrast, neither the Rho kinase inhibitor (Y27632) nor the dominant negative RhoA (DN-RhoA) inhibited angiotensin II-activated fibronectin promoter (Fig. 8C). These results indicate that angiotensin II transactivates the fibronectin gene via the calcium/calmodulin/NFAT pathway but the process is independent of RhoA and Rho kinase.

## DISCUSSION

It has now become a standard clinical care to use the calcineurin inhibitor cyclosporine A in patients with idiopathic FSGS (6). The initial assumption was that cyclosporine A acts solely as an immunosuppressant for T cells, thereby ameliorating podocyte injury indirectly via immunomodulation. However, recent findings raised a possibility that podocyte could be a direct target of calcineurin inhibitors (47). Expressing calcineurin (17) or constitutively active NFAT (73) in podocytes was sufficient to induce proteinuria in mice, accompanied by glomerulosclerosis in the latter. Mutants of TRPC6 that are known to cause familial FSGS in humans were found to induce NFAT activation in cultured podocytes (61). Interestingly, angiotensin II-induced TRPC6 upregulation was mediated by NFAT (48), suggesting a possibility of a positive feedback loop. It was also shown that calcineurin-dependent NFAT activation mediates podocyte apoptosis in diabetic nephropathy (71). Collectively, accumulating data suggest that activation of the calcineurin/NFAT pathway locally in podocytes may contribute to the pathogenesis of proteinuria and glomerulosclerosis. The results of the present studies support this notion and provide a possible mechanism by which the calcineurin/NFAT pathway contributes to the accumulation of the extracellular matrix in the glomerulus (Fig. 9). Further support for nonimmunological actions of calcineurin/NFAT can be found in cardiac myocytes; for example, the calcineurin-NFAT pathway was established as a central mediator of cardiac hypertrophy (40, 75, 80). It should be noted, however, that the response to NFAT activation is highly cell dependent. For example, it was shown that calcineurin/NFAT mediates TGF- $\beta$ -induced fibronectin upregulation in glomerular mesangial

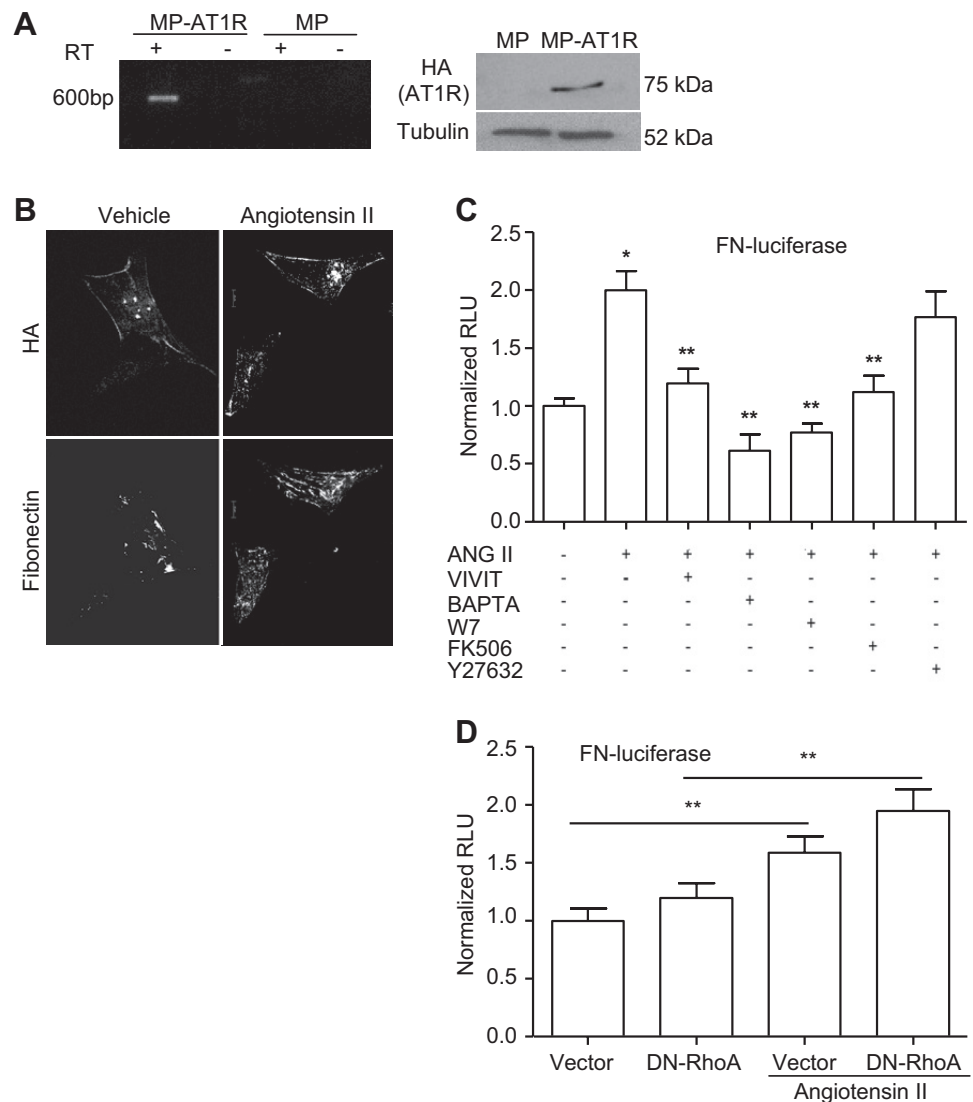


Fig. 8. Angiotensin II-induced fibronectin upregulation is dependent on NFAT but not on Rho kinase. *A*: mouse podocytes were stably transfected with the HA-AT1R plasmid (MP-AT1R). Expression was confirmed by RT-PCR (*left*) and immunoblotting for HA (*right*). *B*: MP-AT1R were stimulated with angiotensin II (ANG II, 0.1  $\mu$ M) or vehicle for 24 h. Fibronectin upregulation was confirmed by immunostaining. Magnification:  $\times 630$ . *C*: MP-AT1R were transfected with FN-luciferase and stimulated with ANG II for 24 h. Inhibitors were added as in Fig. 2;  $n = 6$ . Inhibitors of the calcineurin/NFAT pathway, but not the Rho-kinase inhibitor, inhibited ANG II-induced FN promoter activation. *D*: effect of DN-RhoA was tested as in *C*.

cells while it has the opposite impact in tubular cells (10). Our results definitively identified NFAT as a stimulant of fibronectin production in podocytes in a TGF- $\beta$ -independent manner.

Homeostasis of calcium ion ( $\text{Ca}^{2+}$ ) is essential for cellular function (9). More than a decade ago, it was reported that polycations-induced  $\text{Ca}^{2+}$  influx might be an early event in the pathogenesis of protamine sulfate-mediated retraction of podocyte foot processes (60). More recently,  $\text{Ca}^{2+}$  and related signaling pathways were found to play a critical role in the initial stages of podocyte injury (69). Also, albumin overload was shown to increase intracellular calcium ion concentration ( $[\text{Ca}^{2+}]_i$ ) in podocytes both via the  $\text{Ca}^{2+}$  influx and the release of the intracellular  $\text{Ca}^{2+}$  stores (8). A number of cation channels have been identified to cause  $\text{Ca}^{2+}$  influx in podocytes (16, 35, 58, 68). Among them, TRPC6 has been attracting most attention. TRPC6 is a nonselective cation channel with preference to  $\text{Ca}^{2+}$  (56), and its mutations can cause familial FSGS (58, 77). There have been several reports linking RhoA activation and TRPC6-mediated  $\text{Ca}^{2+}$  influx. In endothelial cells,  $\text{Ca}^{2+}$  influx via TRPC6 channel induced RhoA activation and cell contraction (64). Similarly, Greka and colleagues (68)

demonstrated that TRPC6-mediated  $\text{Ca}^{2+}$  influx induced RhoA activation. In contrast, Henstridge et al. (24) showed that RhoA activates prolonged oscillatory  $\text{Ca}^{2+}$  release from the intracellular stores in HEK293 cells. Thus RhoA and TRPC6-mediated  $\text{Ca}^{2+}$  influx may form a positive feedback loop, as was seen between Rac1 and TRPC5 (22), contributing to podocyte injury.

The present results suggest that RhoA induces a rise of  $[\text{Ca}^{2+}]_i$  which was dependent on the extracellular  $\text{Ca}^{2+}$  (Fig. 7A).  $\text{Ca}^{2+}$  influx was, at least in part, mediated by TRPC6 channels as suggested by the effect of the cation channel inhibitors, SKF-96365 and 2-ABP (Fig. 7A), and TRPC6 knockdown (Fig. 7B). The mechanisms by which RhoA activates TRPC channel(s) are yet to be determined. One possibility is that RhoA modulates the insertion of TRPC6 in the plasma membrane. There have been several reports supporting the role of Rho-GTPases in the membrane insertion of TRPC channels; Rac1 was shown to mediate TRPC5 insertion to the plasma membrane and to initiate  $\text{Ca}^{2+}$  influx (4, 68). Similarly, RhoA facilitated membrane insertion of TRPC6 following the thrombin stimulation in endothelial cells (46) or the Gq pro-

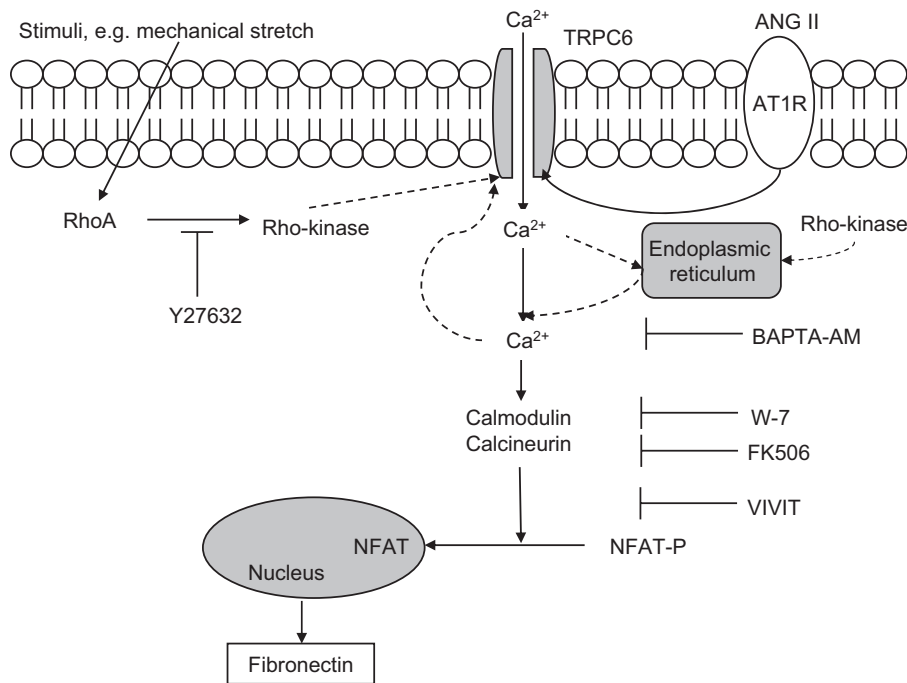


Fig. 9. Proposed pathway for RhoA-mediated fibronectin upregulation in podocytes. Active RhoA modulates TRPC6 via Rho kinase and induces a  $\text{Ca}^{2+}$  influx, which in turn triggers a release of the intracellular  $\text{Ca}^{2+}$  stores. Alternatively, Rho kinase may trigger a release of the intracellular  $\text{Ca}^{2+}$  stores, which in turn induces a  $\text{Ca}^{2+}$  influx. Increase of intracellular  $\text{Ca}^{2+}$  leads to the activation and nuclear translocation of NFAT via the calcium/calcineurin/NFAT signal pathway, stimulating fibronectin transcription and upregulation.

tein-coupled receptor activation in HEK293 cells (7). Also, a proteoglycan, syndecan 4, was shown to enhance the insertion of TRPC6 channels in the plasma membrane via a RhoA-dependent pathway in podocytes (43). Another possibility is that RhoA modulates the channel activities of TRPC6 by posttranslational modifications such as phosphorylation. Phosphorylation of TRPC channels has been shown to regulate channel activities, membrane trafficking, and formation of protein complexes (36). For example, phosphorylation of Y284 of TRPC6 was shown to be necessary for its trafficking to the plasma membrane (32). Of interest, in addition to the acute effect (Fig. 6, B and C), RhoA also induced TRPC6 upregulation after 24 h (Fig. 7C). This suggests that RhoA may not only regulate the TRPC channel localization and/or activity but also their expression level.

Information on the role of RhoA in fibronectin upregulation is limited. Constitutively active RhoA was shown to facilitate the fibronectin matrix formation in renal cancer cells (18). Krepinsky and colleagues demonstrated that RhoA and its downstream kinase, Rho kinase, mediate TGF- $\beta$  (54) and high glucose (53)-mediated fibronectin upregulation in mesangial cells. The transcription factor activator protein-1 was implicated in the latter; however, further mechanisms have not been studied. In the current study, we demonstrated that RhoA-mediated fibronectin upregulation is dependent on the calcium/NFAT signal pathway. This pathway would, at least in part, explain our previous observation that induction of CA-RhoA in podocytes in mice causes histological changes similar to FSGS. In addition, it is established that RhoA is activated when podocytes are mechanically stretched (13). Therefore, stretch-induced RhoA activation is likely to contribute to matrix synthesis and development of glomerulosclerosis secondary to glomerular hypertension as is seen in hypertensive glomerulosclerosis or remnant/hyperfiltrating kidneys. Similarly, the role of mechanical stretch and RhoA activation in the increased matrix production has been also shown in glomerular mesan-

gial cells (31, 79). The potential contributions of other transcription factors downstream of RhoA such as myocardin-related transcription factor (15) or synergy of NFAT with other transcription factors (44) need to be addressed in future studies.

It is firmly established that calcineurin inhibitors, such as cyclosporine A and FK506, are potent inhibitors of the calcineurin-NFAT pathway (41). Thus we were surprised to observe that FK506 did not completely block RhoA-induced NFAT activation or fibronectin activation (Figs. 2C and 4A). Calcineurin inhibitors are known to prevent ubiquitination-mediated protein degradation of RhoA (2). In a recent study, cyclosporine A and cyclosporine/sirolimus combination were found to activate RhoA and actin remodeling in renal tubular epithelia (45). Consistent with these reports, we also observed that when mouse podocyte transfected with CA-RhoA were treated with calcineurin inhibitors, expression of CA-RhoA was markedly augmented (not shown). This augmented CA-RhoA stability/expression may counteract the inhibitory action of FK506 on NFAT activation. Alternatively, we cannot exclude the possibility that calcineurin may have substrates other than NFAT that affect fibronectin gene transactivation. In either case, relative inefficiency of calcineurin inhibitors to block RhoA-mediated NFAT activation suggests that we may need to target NFAT directly, rather than inhibiting calcineurins, to block the NFAT-mediated gene regulations downstream of RhoA in podocytes. This opens up an interesting possibility that NFAT could be a therapeutic target where RhoA activation in podocytes is pathogenic such as hypertensive glomerulosclerosis.

In summary, we demonstrated that activation of RhoA induces a rise of  $[\text{Ca}^{2+}]_i$  in glomerular podocytes. Increased  $[\text{Ca}^{2+}]_i$  leads to the activation of the calcineurin/NFAT pathway, which contributed to fibronectin upregulation. This pathway may be responsible for the pathogenesis of certain glomerular diseases such as idiopathic FSGS and hypertensive glomerulosclerosis.

## GRANTS

The study was supported by the operating grants from the Kidney Foundation of Canada (to T. Takano), Canadian Institute of Health Research (MOP-53335; to T. Takano, MOP-44365, MOP-68929 to S. Nattel) and Quebec Heart and Stroke Foundation (to S. Nattel). T. Takano holds a scholarship from the Fonds de la Recherche en Santé du Québec.

## DISCLOSURES

No conflicts of interest, financial or otherwise, are declared by the author(s).

## AUTHOR CONTRIBUTIONS

Author contributions: L.Z., X.-Y.Q., S.N., and T.T. conception and design of research; L.Z., X.-Y.Q., L.A., F.M., and C.B. performed experiments; L.Z., X.-Y.Q., C.B., and T.T. analyzed data; L.Z., X.-Y.Q., S.N., and T.T. interpreted results of experiments; L.Z. and T.T. prepared figures; L.Z. drafted manuscript; L.Z., F.M., and T.T. edited and revised manuscript; L.Z., X.-Y.Q., L.A., F.M., C.B., S.N., and T.T. approved final version of manuscript.

## REFERENCES

- Aoudjit L, Potapov A, Takano T. Prostaglandin E<sub>2</sub> promotes cell survival of glomerular epithelial cells via the EP4 receptor. *Am J Physiol Renal Physiol* 290: F1534–F1542, 2006.
- Asanuma K, Yanagida-Asanuma E, Faul C, Tomino Y, Kim K, Mundel P. Synaptopodin orchestrates actin organization and cell motility via regulation of RhoA signalling. *Nat Cell Biol* 8: 485–491, 2006.
- Attias O, Jiang R, Aoudjit L, Kawachi H, Takano T. Rac1 contributes to actin organization in glomerular podocytes. *Nephron Exp Nephrol* 114: e93–e106, 2010.
- Bezzarides VJ, Ramsey IS, Kotecha S, Greka A, Clapham DE. Rapid vesicular translocation and insertion of TRP channels. *Nat Cell Biol* 6: 709–720, 2004.
- Burridge K, Wennerberg K. Rho and Rac take center stage. *Cell* 116: 167–179, 2004.
- Cattran DC, Alexopoulos E, Heering P, Hoyer PF, Johnston A, Meyrier A, Ponticelli C, Saito T, Choukroun G, Nachman P, Praga M, Yoshikawa N. Cyclosporin in idiopathic glomerular disease associated with the nephrotic syndrome: workshop recommendations. *Kidney Int* 72: 1429–1447, 2007.
- Cayouette S, Lussier MP, Mathieu EL, Bousquet SM, Boulay G. Exocytotic insertion of TRPC6 channel into the plasma membrane upon Gq protein-coupled receptor activation. *J Biol Chem* 279: 7241–7246, 2004.
- Chen S, He FF, Wang H, Fang Z, Shao N, Tian XJ, Liu JS, Zhu ZH, Wang YM, Wang S, Huang K, Zhang C. Calcium entry via TRPC6 mediates albumin overload-induced endoplasmic reticulum stress and apoptosis in podocytes. *Cell Calcium* 50: 523–529, 2011.
- Clapham DE. Calcium signaling. *Cell* 131: 1047–1058, 2007.
- Cobbs SL, Gooch JL. NFATc is required for TGFβ-mediated transcriptional regulation of fibronectin. *Biochem Biophys Res Commun* 362: 288–294, 2007.
- Crabtree GR, Olson EN. NFAT signaling: choreographing the social lives of cells. *Cell* 109, Suppl: S67–79, 2002.
- Daniel C, Schaub K, Amann K, Lawler J, Hugo C. Thrombospondin-1 is an endogenous activator of TGF-β in experimental diabetic nephropathy in vivo. *Diabetes* 56: 2982–2989, 2007.
- Endlich N, Kress KR, Reiser J, Uttenweiler D, Kriz W, Mundel P, Endlich K. Podocytes respond to mechanical stress in vitro. *J Am Soc Nephrol* 12: 413–422, 2001.
- Fabiato A, Fabiato F. Calcium release from the sarcoplasmic reticulum. *Circ Res* 40: 119–129, 1977.
- Fan L, Sebe A, Peterfi Z, Masszi A, Thirone AC, Rotstein OD, Nakano H, McCulloch CA, Szaszi K, Mucsi I, Kapus A. Cell contact-dependent regulation of epithelial-myofibroblast transition via the rho-rho kinase-phospho-myosin pathway. *Mol Biol Cell* 18: 1083–1097, 2007.
- Fan YY, Kohno M, Nakano D, Ohsaki H, Kobori H, Suwarni D, Ohashi N, Hitomi H, Asanuma K, Noma T, Tomino Y, Fujita T, Nishiyama A. Cilnidipine suppresses podocyte injury and proteinuria in metabolic syndrome rats: possible involvement of N-type calcium channel in podocyte. *J Hypertens* 28: 1034–1043, 2010.
- Faul C, Donnelly M, Merscher-Gomez S, Chang YH, Franz S, Delfgaauw J, Chang JM, Choi HY, Campbell KN, Kim K, Reiser J, Mundel P. The actin cytoskeleton of kidney podocytes is a direct target of the antiproteinuric effect of cyclosporine A. *Nat Med* 14: 931–938, 2008.
- Feijoo-Cuaresma M, Mendez F, Maqueda A, Esteban MA, Naranjo-Suarez S, Castellanos MC, del Cerro MH, Vazquez SN, Garcia-Pardo A, Landazuri MO, Calzada MJ. Inadequate activation of the GTPase RhoA contributes to the lack of fibronectin matrix assembly in von Hippel-Lindau protein-defective renal cancer cells. *J Biol Chem* 283: 24982–24990, 2008.
- Finer G, Schnaper HW, Kanwar YS, Liang X, Lin HY, Hayashida T. Divergent roles of Smad3 and PI3-kinase in murine adriamycin nephropathy indicate distinct mechanisms of proteinuria and fibrogenesis. *Kidney Int* 82: 525–536, 2012.
- Fournes B, Farrah J, Olson M, Lamarche-Vane N, Beauchemin N. Distinct Rho GTPase activities regulate epithelial cell localization of the adhesion molecule CEACAM1: involvement of the CEACAM1 transmembrane domain. *Mol Cell Biol* 23: 7291–7304, 2003.
- Gojo A, Utsunomiya K, Taniguchi K, Yokota T, Ishizawa S, Kanazawa Y, Kurata H, Tajima N. The Rho-kinase inhibitor, fasudil, attenuates diabetic nephropathy in streptozotocin-induced diabetic rats. *Eur J Pharmacol* 568: 242–247, 2007.
- Greka A, Mundel P. Balancing calcium signals through TRPC5 and TRPC6 in podocytes. *J Am Soc Nephrol* 22: 1969–1980, 2011.
- Henger A, Huber T, Fischer KG, Nitschke R, Mundel P, Scholmeyer P, Greger R, Pavenstadt H. Angiotensin II increases the cytosolic calcium activity in rat podocytes in culture. *Kidney Int* 52: 687–693, 1997.
- Henstridge CM, Balenga NA, Ford LA, Ross RA, Waldhoer M, Irving AJ. The GPR55 ligand L-α-lysophosphatidylinositol promotes RhoA-dependent Ca<sup>2+</sup> signaling and NFAT activation. *FASEB J* 23: 183–193, 2009.
- Herman-Edelstein M, Thomas MC, Thallas-Bonke V, Saleem M, Cooper ME, Kantharidis P. Dedifferentiation of immortalized human podocytes in response to transforming growth factor-beta: a model for diabetic podocytopathy. *Diabetes* 60: 1779–1788, 2011.
- Hidaka T, Suzuki Y, Yamashita M, Shibata T, Tanaka Y, Horikoshi S, Tomino Y. Amelioration of crescentic glomerulonephritis by RhoA kinase inhibitor, Fasudil, through podocyte protection and prevention of leukocyte migration. *Am J Pathol* 172: 603–614, 2008.
- Hill AJ, Hinton JM, Cheng H, Gao Z, Bates DO, Hancox JC, Langton PD, James AF. A TRPC-like non-selective cation current activated by alpha 1-adrenoceptors in rat mesenteric artery smooth muscle cells. *Cell Calcium* 40: 29–40, 2006.
- Hsu HH, Hoffmann S, Endlich N, Velic A, Schwab A, Weide T, Schlatter E, Pavenstadt H. Mechanisms of angiotensin II signaling on cytoskeleton of podocytes. *J Mol Med* 86: 1379–1394, 2008.
- Im SH, Rao A. Activation and deactivation of gene expression by Ca<sup>2+</sup>/calcineurin-NFAT-mediated signaling. *Mol Cells* 18: 1–9, 2004.
- Inoue R, Okada T, Onoue H, Hara Y, Shimizu S, Naitoh S, Ito Y, Mori Y. The transient receptor potential protein homologue TRP6 is the essential component of vascular alpha(1)-adrenoceptor-activated Ca(2+)-permeable cation channel. *Circ Res* 88: 325–332, 2001.
- Ishida T, Haneda M, Maeda S, Koya D, Kikkawa R. Stretch-induced overproduction of fibronectin in mesangial cells is mediated by the activation of mitogen-activated protein kinase. *Diabetes* 48: 595–602, 1999.
- Kanda S, Harita Y, Shibagaki Y, Sekine T, Igarashi T, Inoue T, Hattori S. Tyrosine phosphorylation-dependent activation of TRPC6 regulated by PLC-γ and nephrin: effect of mutations associated with focal segmental glomerulosclerosis. *Mol Biol Cell* 22: 1824–1835, 2011.
- Kanda T, Wakino S, Hayashi K, Homma K, Ozawa Y, Saruta T. Effect of fasudil on Rho-kinase and nephropathy in subtotal nephrectomized spontaneously hypertensive rats. *Kidney Int* 64: 2009–2019, 2003.
- Kang YS, Li Y, Dai C, Kiss LP, Wu C, Liu Y. Inhibition of integrin-linked kinase blocks podocyte epithelial-mesenchymal transition and ameliorates proteinuria. *Kidney Int* 78: 363–373, 2010.
- Kim EY, Alvarez-Baron CP, Dryer SE. Canonical transient receptor potential channel (TRPC)3 and TRPC6 associate with large-conductance Ca<sup>2+</sup>-activated K<sup>+</sup> (BKCa) channels: role in BKCa trafficking to the surface of cultured podocytes. *Mol Pharmacol* 75: 466–477, 2009.

36. Kiselyov K, Patterson RL. The integrative function of TRPC channels. *Front Biosci* 14: 45–58, 2009.
37. Lee BH, Park SY, Kang KB, Park RW, Kim IS. NF-kappaB activates fibronectin gene expression in rat hepatocytes. *Biochem Biophys Res Commun* 297: 1218–1224, 2002.
38. Li JJ, Kwak SJ, Jung DS, Kim JJ, Yoo TH, Ryu DR, Han SH, Choi HY, Lee JE, Moon SJ, Kim DK, Han DS, Kang SW. Podocyte biology in diabetic nephropathy. *Kidney Int Suppl* S36–42, 2007.
39. Li Y, Kang YS, Dai C, Kiss LP, Wen X, Liu Y. Epithelial-to-mesenchymal transition is a potential pathway leading to podocyte dysfunction and proteinuria. *Am J Pathol* 172: 299–308, 2008.
40. Lin Z, Murtaza I, Wang K, Jiao J, Gao J, Li PF. miR-23a functions downstream of NFATc3 to regulate cardiac hypertrophy. *Proc Natl Acad Sci USA* 106: 12103–12108, 2009.
41. Liu J, Farmer JD Jr, Lane WS, Friedman J, Weissman I, Schreiber SL. Calcineurin is a common target of cyclophilin-cyclosporin A and FKBP-FK506 complexes. *Cell* 66: 807–815, 1991.
42. Liu Y. New insights into epithelial-mesenchymal transition in kidney fibrosis. *J Am Soc Nephrol* 21: 212–222, 2010.
43. Liu Y, Echtermeier F, Thilo F, Theilmeier G, Schmidt A, Schulein R, Jensen BL, Loddikenemper C, Jankowski V, Marcussen N, Gollasch M, Arendshorst WJ, Tepel M. The proteoglycan syndecan 4 regulates transient receptor potential canonical 6 channels via RhoA/Rho-associated protein kinase signaling. *Arterioscler Thromb Vasc Biol* 32: 378–385, 2012.
44. Macian F, Lopez-Rodriguez C, Rao A. Partners in transcription: NFAT and AP-1. *Oncogene* 20: 2476–2489, 2001.
45. Martin-Martin N, Dan Q, Amoozadeh Y, Waheed F, McMorrow T, Ryan MP, Szasz K. RhoA and Rho kinase mediate cyclosporine A and sirolimus-induced barrier tightening in renal proximal tubular cells. *Int J Biochem Cell Biol* 44: 178–188, 2012.
46. Mehta D, Ahmed GU, Paria BC, Holinstat M, Voyno-Yasenetskaya T, Tirupathi C, Minshall RD, Malik AB. RhoA interaction with inositol 1,4,5-trisphosphate receptor and transient receptor potential channel-1 regulates Ca<sup>2+</sup> entry. Role in signaling increased endothelial permeability. *J Biol Chem* 278: 33492–33500, 2003.
47. Meyrier AY. Treatment of focal segmental glomerulosclerosis with immunophilin modulation: when did we stop thinking about pathogenesis? *Kidney Int* 76: 487–491, 2009.
48. Nijenhuis T, Sloan AJ, Hoenderop JG, Flesche J, van Goor H, Kistler AD, Bakker M, Binders RJ, de Boer RA, Moller CC, Hamming I, Navis G, Wetzels JF, Berden JH, Reiser J, Faul C, van der Vlag J. Angiotensin II contributes to podocyte injury by increasing TRPC6 expression via an NFAT-mediated positive feedback signaling pathway. *Am J Pathol* 179: 1719–1732, 2011.
49. Nishida K, Qi XY, Wakili R, Comtois P, Chartier D, Harada M, Iwasaki YK, Romeo P, Maguy A, Dobrev D, Michael G, Talajic M, Nattel S. Mechanisms of atrial tachyarrhythmias associated with coronary artery occlusion in a chronic canine model. *Circulation* 123: 137–146, 2011.
50. Noguchi H, Matsushita M, Okitsu T, Moriwaki A, Tomizawa K, Kang S, Li ST, Kobayashi N, Matsumoto S, Tanaka K, Tanaka N, Matsui H. A new cell-permeable peptide allows successful allogeneic islet transplantation in mice. *Nat Med* 10: 305–309, 2004.
51. Northrop JP, Ho SN, Chen L, Thomas DJ, Timmerman LA, Nolan GP, Admon A, Crabtree GR. NF-AT components define a family of transcription factors targeted in T-cell activation. *Nature* 369: 497–502, 1994.
52. Parekh AB, Putney JW Jr. Store-operated calcium channels. *Physiol Rev* 85: 757–810, 2005.
53. Peng F, Wu D, Gao B, Ingram AJ, Zhang B, Chorneyko K, McKenzie R, Krepinsky JC. RhoA/Rho-kinase contribute to the pathogenesis of diabetic renal disease. *Diabetes* 57: 1683–1692, 2008.
54. Peng F, Zhang B, Wu D, Ingram AJ, Gao B, Krepinsky JC. TGFbeta-induced RhoA activation and fibronectin production in mesangial cells require caveolae. *Am J Physiol Renal Physiol* 295: F153–F164, 2008.
55. Phillips LM, Wang Y, Dai T, Feldman DL, LaPage J, Adler SG. The renin inhibitor aliskiren attenuates high-glucose induced extracellular matrix synthesis and prevents apoptosis in cultured podocytes. *Nephron Exp Nephrol* 118: e49–59, 2011.
56. Ramsey IS, Delling M, Clapham DE. An introduction to TRP channels. *Annu Rev Physiol* 68: 619–647, 2006.
57. Rao A, Luo C, Hogan PG. Transcription factors of the NFAT family: regulation and function. *Annu Rev Immunol* 15: 707–747, 1997.
58. Reiser J, Polu KR, Moller CC, Kenlan P, Altintas MM, Wei C, Faul C, Herbert S, Villegas I, Avila-Casado C, McGee M, Sugimoto H, Brown D, Kalluri R, Mundel P, Smith PL, Clapham DE, Pollak MR. TRPC6 is a glomerular slit diaphragm-associated channel required for normal renal function. *Nat Genet* 37: 739–744, 2005.
59. Richardson CA, Gordon KL, Couser WG, Bomsztyk K. IL-1β increases laminin B2 chain mRNA levels and activates NF-κB in rat glomerular epithelial cells. *Am J Physiol Renal Physiol* 268: F273–F278, 1995.
60. Rudiger F, Greger R, Nitschke R, Henger A, Mundel P, Pavenstadt H. Polycations induce calcium signaling in glomerular podocytes. *Kidney Int* 56: 1700–1709, 1999.
61. Schlondorff J, Del Camino D, Carrasquillo R, Lacey V, Pollak MR. TRPC6 mutations associated with focal segmental glomerulosclerosis cause constitutive activation of NFAT-dependent transcription. *Am J Physiol Cell Physiol* 296: C558–C569, 2009.
62. Shankland SJ. The podocyte's response to injury: role in proteinuria and glomerulosclerosis. *Kidney Int* 69: 2131–2147, 2006.
63. Shibata S, Nagase M, Fujita T. Fluvastatin ameliorates podocyte injury in proteinuric rats via modulation of excessive Rho signaling. *J Am Soc Nephrol* 17: 754–764, 2006.
64. Singh I, Knezevic N, Ahmed GU, Kini V, Malik AB, Mehta D. Galphaq-TRPC6-mediated Ca<sup>2+</sup> entry induces RhoA activation and resultant endothelial cell shape change in response to thrombin. *J Biol Chem* 282: 7833–7843, 2007.
65. Spletstoeser F, Florea AM, Busseberg D. IP(3) receptor antagonist, 2-APB, attenuates cisplatin induced Ca<sup>2+</sup>-influx in HeLa-S3 cells and prevents activation of calpain and induction of apoptosis. *Br J Pharmacol* 151: 1176–1186, 2007.
66. Takano T, Cybulsky AV. Complement C5b-9-mediated arachidonic acid metabolism in glomerular epithelial cells: role of cyclooxygenase-1 and -2. *Am J Pathol* 156: 2091–2101, 2000.
67. Takano T, Cybulsky AV, Yang X, Aoudjit L. Complement C5b-9 induces cyclooxygenase-2 gene transcription in glomerular epithelial cells. *Am J Physiol Renal Physiol* 281: F841–F850, 2001.
68. Tian D, Jacobo SM, Billing D, Rozkalne A, Gage SD, Agnostou T, Pavenstadt H, Hsu HH, Schlondorff J, Ramos A, Greka A. Antagonistic regulation of actin dynamics and cell motility by TRPC5 and TRPC6 channels. *Sci Signal* 3: ra77, 2010.
69. Vassiliadis J, Bracken C, Matthews D, O'Brien S, Schiavi S, Wawersik S. Calcium mediates glomerular filtration through calcineurin and mTORC2/Akt signaling. *J Am Soc Nephrol* 22: 1453–1461, 2011.
70. Veron D, Villegas G, Aggarwal PK, Bertuccio C, Jimenez J, Velazquez H, Reidy K, Abrahamson DR, Moeckel G, Kashgarian M, Tufo A. Acute podocyte vascular endothelial growth factor (VEGF-A) knockdown disrupts alpha(v)beta(3) integrin signaling in the glomerulus. *PLoS One* 7: e40589, 2012.
71. Wang L, Chang JH, Paik SY, Tang Y, Eisner W, Spurney RF. Calcineurin (CN) activation promotes apoptosis of glomerular podocytes both in vitro and in vivo. *Mol Endocrinol* 25: 1376–1386, 2011.
72. Wang W, Wang Y, Long J, Wang J, Haudek SB, Overbeek P, Chang BH, Schumacker PT, Danesh FR. Mitochondrial fission triggered by hyperglycemia is mediated by ROCK1 activation in podocytes and endothelial cells. *Cell Metab* 15: 186–200, 2012.
73. Wang Y, Jarad G, Tripathi P, Pan M, Cunningham J, Martin DR, Liapis H, Miner JH, Chen F. Activation of NFAT signaling in podocytes causes glomerulosclerosis. *J Am Soc Nephrol* 21: 1657–1666, 2010.
74. Wiggins RC. The spectrum of podocytopathies: a unifying view of glomerular diseases. *Kidney Int* 71: 1205–1214, 2007.
75. Wilkins BJ, Dai YS, Bueno OF, Parsons SA, Xu J, Plank DM, Jones F, Kimball TR, Molkenin JD. Calcineurin/NFAT coupling participates in pathological, but not physiological, cardiac hypertrophy. *Circ Res* 94: 110–118, 2004.
76. Winn MP. Approach to the evaluation of heritable diseases and update on familial focal segmental glomerulosclerosis. *Nephrol Dial Transplant* 18, Suppl 6: vi14–20, 2003.
77. Winn MP, Conlon PJ, Lynn KL, Farrington MK, Creazzo T, Hawkins AF, Daskalakis N, Kwan SY, Ebersviller S, Burchette JL, Pericak-Vance MA, Howell DN, Vance JM, Rosenberg PB. A mutation in the TRPC6 cation channel causes familial focal segmental glomerulosclerosis. *Science* 308: 1801–1804, 2005.

78. **Wu S, Jian MY, Xu YC, Zhou C, Al-Mehdi AB, Liedtke W, Shin HS, Townsley MI.**  $\text{Ca}^{2+}$  entry via  $\alpha_{1G}$  and TRPV4 channels differentially regulates surface expression of P-selectin and barrier integrity in pulmonary capillary endothelium. *Am J Physiol Lung Cell Mol Physiol* 297: L650–L657, 2009.
79. **Yasuda T, Kondo S, Homma T, Harris RC.** Regulation of extracellular matrix by mechanical stress in rat glomerular mesangial cells. *J Clin Invest* 98: 1991–2000, 1996.
80. **Yu H, van Berkel TJ, Biessen EA.** Therapeutic potential of VIVIT, a selective peptide inhibitor of nuclear factor of activated T cells, in cardiovascular disorders. *Cardiovasc Drug Rev* 25: 175–187, 2007.
81. **Zhang H, Cybulsky AV, Aoudjit L, Zhu J, Li H, Lamarche-Vane N, Takano T.** Role of Rho-GTPases in complement-mediated glomerular epithelial cell injury. *Am J Physiol Renal Physiol* 293: F148–F156, 2007.
82. **Zhu L, Jiang R, Aoudjit L, Jones N, Takano T.** Activation of RhoA in podocytes induces focal segmental glomerulosclerosis. *J Am Soc Nephrol* 22: 1621–1630, 2011.
83. **Ziembicki J, Tandon R, Schelling JR, Sedor JR, Miller RT, Huang C.** Mechanical force-activated phospholipase D is mediated by  $\text{G}\alpha_{12/13}$ -Rho and calmodulin-dependent kinase in renal epithelial cells. *Am J Physiol Renal Physiol* 289: F826–F834, 2005.
84. **Zimmerman B, Simaan M, Lee MH, Luttrell LM, Laporte SA.** c-Src-mediated phosphorylation of AP-2 reveals a general mechanism for receptors internalizing through the clathrin pathway. *Cell Signal* 21: 103–110, 2009.
85. **Ziyadeh FN, Wolf G.** Pathogenesis of the podocytopathy and proteinuria in diabetic glomerulopathy. *Curr Diabetes Rev* 4: 39–45, 2008.

